Tellus (1997), 49B, 149–158
Printed in UK – all rights reserved

TELLUS
ISSN 0280–6509

The effect of rain on air-water gas exchange

By DAVID T. HO[1]*, LARRY F. BLIVEN[2], RIK WANNINKHOF[3] and PETER SCHLOSSER[1],
[1]*Lamont-Doherty Earth Observatory and Department of Earth and Environmental Sciences, Columbia University, Palisades, NY 10964, USA;* [2]*NASA/GSFC, Laboratory for Hydrospheric Processes, Wallops Island, VA 23337, USA;* [3]*NOAA/AOML, Ocean Chemistry Division, Miami, FL 33149, USA*

(Manuscript received 23 September 1996; in final form 9 December 1996)

ABSTRACT

The relationship between gas transfer velocity and rain rate was investigated at NASA's Rain-Sea Interaction Facility (RSIF) using several SF_6 evasion experiments. During each experiment, a water tank below the rain simulator was supersaturated with SF_6, a synthetic gas, and the gas transfer velocities were calculated from the measured decrease in SF_6 concentration with time. The results from experiments with 18 different rain rates (7 to 110 mm h^{-1}) and 1 of 2 dropsizes (2.8 or 4.2 mm diameter) confirm a significant and systematic enhancement of air-water gas exchange by rainfall. The gas transfer velocities derived from our experiment were related to the kinetic energy flux calculated from the rain rate and dropsize. The relationship obtained for mono-dropsize rain at the RSIF was extrapolated to natural rain using the kinetic energy flux of natural rain calculated from the Marshall-Palmer raindrop size distribution. Results of laboratory experiments at RSIF were compared to field observations made during a tropical rainstorm in Miami, Florida and show good agreement between laboratory and field data.

1. Introduction

Exchange of gases across the air-water interface influences many properties of natural waters. Knowledge of this parameter is critical for evaluating indicators of water quality (e.g., dissolved oxygen = DO) (Odum, 1956; O'Connor, 1962; Clark et al., 1995b), understanding cycling of biogeochemically important trace gases (e.g., CO_2, CH_4, DMS, N_2O, CH_3Br) (Broecker et al., 1985; Bates et al., 1993; Yvon and Butler, 1996), and predicting evasion rates of volatile pollutants (e.g., toxic halogenated compounds) (Bopp, 1983; Dyrssen et al., 1990; Thomann et al., 1991; McConnell et al., 1993).

Over large water bodies such as oceans or large lakes, gas exchange is governed primarily by wind driven turbulence on the water surface and, to a lesser extent, by air bubble entrainment (Merlivat and Memery, 1983; Jähne et al., 1987). However, on the local scale of rivers, small lakes, estuaries, and wetlands, other factors contribute significantly to the turbulence regime, especially at low wind speeds (Livingstone and Imboden, 1993; Clark et al., 1995a). One of these factors is rain falling onto the water surface.

Relatively little experimental work has been directed at quantifying the influence of rainfall on air-water gas exchange. Bopp et al. (1981) speculated that rain might have been responsible for rapid gas exchange observed during a gas-exchange experiment in a model estuarine ecosystem. For light rains (<25 mm h^{-1}), some exploratory laboratory (Banks et al., 1984) and field experiments (Belanger and Korzun, 1991) suggest a power law and linear relationship,

* Corresponding author.

respectively, between oxygen exchange and rain rate. Presently, because the number of laboratory experimental points is small, and interpretation of field data is hampered by variable rainfall rates during rain storms, no generally accepted relationship exists between gas exchange and rain rate.

Here, we present a first-order relationship between gas transfer velocity and rain rate based on laboratory experiments carried out at the Rain-Sea Interaction Facility (RSIF) (Bliven and Elfouhaily, 1993) located at NASA/GSFC Wallops Flight Facility (WFF) in Wallops Island, Virginia. Gas transfer velocities for sulfur hexafluoride (SF_6) were determined for various rain rates and drop-sizes. The kinetic energy flux of the simulated rain was then calculated and related to the gas transfer velocity. Furthermore, the gas transfer velocity was related to natural rain by calculating the kinetic energy flux of natural rain from the Marshall-Palmer (henceforth called MP) raindrop size distribution (Marshall and Palmer, 1948). Finally, the laboratory data from RSIF was compared to field data collected in Miami, Florida. The agreement between laboratory and field data supports both our relationship between kinetic energy flux and gas transfer velocity and the extrapolation to natural rain using the Marshall-Palmer raindrop size distribution.

2. Principle of the SF_6 evasion method

Sulfur hexafluoride (SF_6), a synthetic gas, was chosen as the tracer in the present experiment because it can be measured at very low concentrations, it is chemically and biologically inert in water, and its background concentration in water ($\sim$0.03 parts per trillion by volume (pptv)) is below our detection limit ($\sim$0.5 pptv). Combining these properties with its low solubility in water (Ostwald solubility coefficient $\alpha=0.0058$ at 25°C; Wanninkhof, 1992), very little SF_6 is needed to raise the levels in the water far above background concentrations.

The principle of the SF_6 evasion experiments used in this study is the same as that applied in previous gas exchange experiments conducted with SF_6 in closed systems (e.g., lakes, wind tunnels (Wanninkhof et al., 1985; Upstill-Goddard et al., 1990; Wanninkhof and Bliven, 1991; Clark et al., 1995a)) and described in detail by Wanninkhof et al. (1987). First, SF_6 is injected into a water body. The decrease in the SF_6 concentration is then measured and converted into a gas transfer velocity k, which is defined as:

$$k=\frac{F_k}{C_w-\alpha C_a} \tag{1}$$

where F_k is the flux of SF_6, C_w is the SF_6 concentration below the air-water interface, C_a is the SF_6 concentration in the air and α is the Ostwald solubility coefficient. F_k can be written as:

$$F_k=\frac{1}{A}\frac{dM}{dt}, \tag{2}$$

where M is the total mass of SF_6 in the water, and A is the surface area of the water body. If the water is well mixed:

$$F_k=h\frac{dC}{dt}, \tag{3}$$

where C is the average SF_6 concentration in the water, and h is the mean depth of the water. Combining eqs. (1) and (3) while setting $C_w=C$ and integrating between t_i and t_f yields:

$$k=\frac{h}{\Delta t}\ln\left(\frac{C_i-\alpha C_a}{C_f-\alpha C_a}\right) \tag{4}$$

where C_i and C_f are the average SF_6 concentrations at t_i and t_f, respectively, and $\Delta t=t_f-t_i$. Since both C_i and C_f are much greater than αC_a, we can neglect the latter term and thus express k as:

$$k=\frac{h}{\Delta t}\ln\frac{C_i}{C_f}. \tag{5}$$

3. Experimental setup and methods

3.1. *Rain-Sea Interaction Facility (RSIF)*

The RSIF, a $4\times4\times17$ m tower, is designed to simulate rain. Its height allows falling water droplets to approach terminal velocity before impacting the water surface below. The velocity of 2.8 mm drops was measured to be 7.80 m s^{-1} at the RSIF by Sobieski and Bliven (1995), which is within 1% of its terminal velocity (terminal velocity = 7.82 and 8.92 m s^{-1} for 2.8 and 4.2 mm drops respectively; Gunn and Kinzer, 1949). A rain

simulator ($80 \times 80 \times 6$ cm), with 1100 nozzles and 2.5 cm center point spacing, is suspended from the catwalk (13 m high) of the tower. It can generate a broad range of rain rates (R), from 5 to 120 mm h^{-1}, with dropsize diameters (D) ranging from 1.2 to 4.2 mm. The dropsize is controlled by attaching different gauge hypodermic needles to the nozzles. At ground level, there is a tank ($200 \times 140 \times 80$ cm) which receives the water from the rain simulator. In the same tower, next to the rain water tank, there is an identical water tank, sheltered from the rain by a tarp 3 m overhead, which was used for the control experiments.

3.2. *SF_6 injection, sample collection, and measurement*

At the beginning of each experiment, the rain water tank was filled with filtered tap water to the desired volume. Then, the tank water was supersaturated with SF_6 by injecting a predetermined amount of SF_6 ($\sim 4.6 \times 10^{-9}$ moles) dissolved in water with a 1 ml syringe. The water in the tank was mixed until the difference in SF_6 concentration measured at different parts of the tank was no greater than the precision of the analytical method ($\pm 2\%$). At this point, the rain simulator was turned on and tank water samples were taken to establish initial conditions. The tank was configured in one of two modes: (1) with overflow and (2) without overflow. In the first configuration, a hose, connected to the drain at the bottom of the tank, was extended upward for use as a water overflow outlet to keep the water level in the tank (and thus the volume) constant. In the other configuration, the drain was plugged and no water was allowed to escape, causing the water level (and volume) in the tank to increase with time. The gas transfer velocity was determined by measuring the SF_6 concentration decrease with time, with a correction applied for dilution in both configurations.

The control water tank was filled and injected with SF_6 in the same way as the tank used for the SF_6 evasion experiments. Because the gas transfer velocity was very low for the control experiments, only one injection was necessary for the duration of all rain experiments. At the beginning of each experiment, the water surface of the control tank was skimmed for surfactants. The gas transfer velocity for no rain conditions ($R = 0$) was determined by measuring the decrease in SF_6 concentration with time in the control water tank.

The water samples were collected in 50 ml glass syringes and analyzed using a headspace method described in detail by Wanninkhof et al. (1987). Glass syringes were filled to a predetermined volume of water (10 to 40 ml, depending on the expected SF_6 concentration) and then a headspace of known volume (40 to 10 ml) was created with ultra-high purity (UHP) N_2. After at least 3 min of vigorous shaking on a mechanical shaker to equilibrate the water with the N_2 in the headspace, the sample was pushed through a drying column of $Mg(ClO_4)_2$ into a sample loop. Subsequently, the sample was injected into a gas chromatograph (Shimadzu 8A) equipped with an electron capture detector (ECD) by UHP N_2 carrier gas. The SF_6 was separated from other gases at room temperature with a molecular sieve 5a column.

Multiple samples were collected every ten minutes over a period of three to five hours depending on the rain rate and dropsize. A concentration decrease of at least 80% was achieved for each run. During each experiment, samples were drawn from 3 or 4 different depths in the tank. Typically, the SF_6 concentrations of samples from different depths did not vary by more than 3%. Average values of all samples collected at a particular time were used to calculate the gas transfer velocity k.

3.3. *Rain rates and dropsizes*

In this study, the rain rate was calculated from the rate of water delivery from the pump to the rain simulator. For a given pumping rate P (ml min^{-1}), the rain rate R (mm h^{-1}) was calculated as follows:

$$R = 600 \frac{P}{A}, \tag{6}$$

where A is the surface area of the water tank in cm^2 and 600 is the conversion from ml min^{-1} to mm cm^{-2} h^{-1}. It was estimated that at the highest rain rates, 5% of the rain fell outside the water tank below. The pump was calibrated by specifying a desired output volume of water in a given time and weighing the water on a balance to determine the actual volume. The procedure was repeated three times at the beginning and end of each experiment, and the average value was

used to determine the actual pumping rate and thus the rain rate. The average difference between specified and actual pumping rates was 3%. Dropsizes were estimated by weighing the droplets from the nozzles or needles and assuming a spherical shape (Sobieski and Bliven, 1995).

3.4. Dilution models

The observed decrease in SF_6 concentration in the tank during the experiments is caused by two factors: (1) gas exchange at the air-water interface and (2) dilution. We have to quantify the dilution effect in order to calculate the gas transfer velocity k. For the configuration with overflow, the total change in mean SF_6 concentration C in the tank water with time can be described by:

$$h\frac{dC}{dt}=F_k+F_d, \tag{7}$$

where F_k is the gas flux due to gas-exchange, and F_d is the dilution term.

If the concentration in the water C is much greater than the equilibrium concentration with the overlaying air, αC_a, the flux of SF_6 due to gas exchange can be described as follows (Wanninkhof et al., 1985; Wanninkhof et al., 1987):

$$F_k=kC. \tag{8}$$

When the tank was kept at constant volume V by overflow, the dilution can be calculated in the following way:

$$F_d=h\frac{P}{V}C, \tag{9}$$

where P denotes the pumping rate. Combining eqs. (7)–(9), we obtain:

$$h\frac{dC}{dt}=kC+h\frac{P}{V}C. \tag{10}$$

After rearranging eq. 10 and integrating from t_i to t_f, we get:

$$k=\frac{h}{\Delta t}\ln\left(\frac{C_i}{C_f}-\frac{P}{V}\right), \tag{11}$$

where C_i and C_f are the initial and final mean SF_6 concentrations in the tank.

For the case with no overflow of water during the experiment, the following dilution correction has to be applied to the measured concentration C_m:

$$C=\frac{V_0}{(V_0+P\Delta t)}C_m, \tag{12}$$

where V_0 is the volume at time t_0. Then, the transfer velocity k can be derived following Wanninkhof et al. (1987):

$$k=\frac{h}{\Delta t}\ln\frac{C_i}{C_f}, \tag{13}$$

where C_i and C_f are the initial and final dilution-corrected, average SF_6 concentrations in the tank.

The overflow-dilution model (eq. (11)) describes a change in mean SF_6 concentration C in the tank with time and contains no information on spatial variability of SF_6 in the tank. It assumes that the mixing time for SF_6 in the water is much shorter than its mean residence time. To test the validity of this assumption, we replaced SF_6 with salt in our experimental setup as its concentration decrease is due to dilution only. Several kilograms of salt were dissolved in the tank water and the subsequent decrease in salinity with time was measured and compared to the results of the overflow-dilution model. The experimental data were in good agreement with the model predictions.

4. Results

Experiments were conducted using 18 different rain rates (7 to 110 mm h^{-1}) and 1 of 2 dropsizes (2.8 or 4.2 mm diameter). To minimize potential systematic errors, the experiments were carried out using both configurations, i.e., with and without overflow. During each experiment, the SF_6 concentration decreased as a result of both gas exchange and dilution (Fig. 1). The contribution of dilution to the total decrease in SF_6 concentration varied from 10% to 20%, depending on the rain rate and dropsize.

The gas transfer velocities calculated from eqs. 11 (overflow) and 13 (no overflow) were normalized to a Schmidt number (Sc) of 600, corresponding to values for CO_2 at 20°C (Sc = kinematic viscosity of water divided by the molecular diffusivity of the gas in water) and assuming that k is

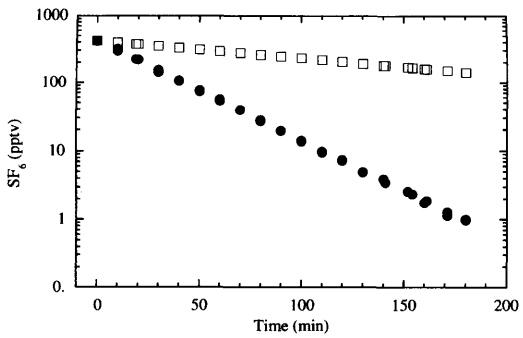

Fig. 1. SF_6 concentration as a function of time during a typical experiment (log scale). The rain rate for this experiment was 82.2 mm h^{-1} with 4.2 mm drops corresponding to a KEF of 0.91 J m^{-2} s^{-1}. Open squares = dilution (model) and filled circles = gas exchange plus dilution (measured). Gas exchange and dilution contributed 82% and 18% to the observed decrease in SF_6 concentration, respectively.

proportional to $Sc^{-1/2}$ (Jähne et al., 1987) as follows:

$$k(600) = k_{SF_6}\left(\frac{Sc_{SF_6}}{600}\right)^{-\frac{1}{2}}, \qquad (14)$$

where k_{SF_6} is the gas transfer velocity for SF_6, and Sc_{SF_6} is the Schmidt number of SF_6 calculated from the diffusion coefficient of King and Saltzman (1995).

When gas transfer is correlated with rain rates, similar trends are observed for both the 2.8 and 4.2 mm dropsizes (Fig. 2a). The gas transfer velocity increases rapidly and almost linearly up to rain rates of about 50 mm h^{-1} for both dropsizes. Above 50 mm h^{-1}, there is still a strong dependence of gas exchange on the rain rate for the 4.2 mm dropsize but the effect is not as dramatic as for lower rain rates. Experiments with rain rates above 50 mm h^{-1} were conducted only with 4.2 mm dropsize rain because it is difficult to maintain discrete 2.8 mm rain droplets with the rain simulator above 50 mm h^{-1}. Intuitively, one would expect the 4.2 mm raindrops to have a greater effect on gas exchange. Experiments with similar rain rates but different dropsizes show that enhancement of gas exchange using the 2.8 mm drops is typically 83% of that achieved with 4.2 mm drops (Table 1). Gas exchange with $R = 0$ was 0.35 cm h^{-1} over the period of the rain experiments as determined from the control experiment.

To combine the data sets for 2.8 and 4.2 mm raindrops, we computed the kinetic energy flux (KEF) of the simulated rain in order to relate the gas transfer rate to a single parameter. The kinetic energy E_k of the droplets is given by:

$$E_k = \tfrac{1}{2}mv^2 = \tfrac{1}{2}\rho V v^2, \qquad (15)$$

where ρ is the density of the raindrops, V is the volume of the raindrops and v is the terminal velocity of the droplets as measured by Gunn and Kinzer (1949). Accordingly, the kinetic energy flux of the rain droplets is:

$$\mathrm{KEF} = \frac{E_k}{At} = \tfrac{1}{2}\rho V n v^2 = \tfrac{1}{2}\rho R v^2, \qquad (16)$$

where A is the surface area of the water tank, n is the number of drops crossing A during the time

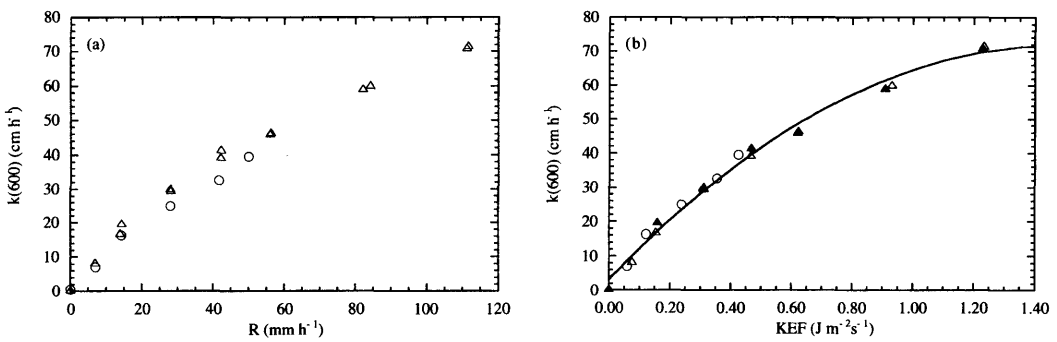

Fig. 2. (a) Relationship between rain rate R and gas transfer velocity $k(600)$. Circles = 2.8 mm drops; triangles = 4.2 mm drops. Enhancement due to 2.8 mm drops is typically 83% of 4.2 mm drops. (b) Relationship between kinetic energy flux KEF and gas transfer velocity $k(600)$. Filled symbols = experiments with overflow; open symbols = experiments with no overflow; circles = 2.8 mm drops; triangles = 4.2 mm drops. The 2nd order polynomial fit to the data points is $k(600) = 2.48 + 65.46\ \mathrm{KEF} - 21.81\ \mathrm{KEF}^2$ ($r^2 = 0.992$).

Table 1. *Results of experiments at RSIF*

Rain rate (mm h^{-1})	Drop size (mm)	KEF (J m^{-2} s^{-1})	$k(600)$ (cm h^{-1})	Overflow
0.00	—	0.00	0.49	no
6.90	4.2	0.08	8.41	no
7.05	2.8	0.06	7.00	no
13.97	4.2	0.15	17.01	no
14.26	2.8	0.12	16.27	no
14.35	4.2	0.16	19.80	yes
28.05	2.8	0.24	24.91	no
28.06	4.2	0.31	30.12	no
28.14	4.2	0.31	29.63	yes
41.64	2.8	0.35	32.54	no
42.16	4.2	0.47	39.39	no
42.25	4.2	0.47	41.61	yes
49.97	2.8	0.42	39.56	no
56.06	4.2	0.62	46.04	no
56.28	4.2	0.62	46.54	yes
82.18	4.2	0.91	59.26	yes
84.22	4.2	0.93	60.22	no
111.19	4.2	1.23	71.07	yes
111.61	4.2	1.23	71.72	no

interval t, and $R=nV$. Hence, for the same rain rate, the KEF for the 4.2 mm drops is about 31% higher than for the 2.8 mm drops.

The combined results of the various experiments (Table 1, Fig. 2b) show that gas transfer velocities of the two dropsizes become indistinguishable when expressed in terms of KEF. The relationship between $k(600)$ and KEF can be characterized by the following 2nd order polynomial:

$$k(600)=2.48+65.46\mathrm{KEF}-21.81\mathrm{KEF}^2 \quad (r^2=0.992). \tag{17}$$

Further experiments covering a large spectrum of raindrop sizes will be necessary to firmly establish this relationship. In the KEF range investigated in our experiment, $k(600)$ ranged from 0.5 to 71.7 cm h^{-1} and the highest $k(600)$ corresponds to a short-term wind speed, corrected to a height of 10 m (U_{10}), of about 15 m s^{-1} (Wanninkhof, 1992).

5. Discussion

5.1. *Relationship between natural rain and gas exchange*

Since the rainfall rate is the most widely used parameter for characterizing rain events in nature, it is useful to establish a correlation between natural rain rate R_n and $k(600)$. We cannot relate our mono-dropsize rain rate R (for either the 2.8 or 4.2 mm drops) directly to natural rain because unlike our simulated rain at RSIF, natural rain has a spectrum of dropsizes and the raindrop size distribution (RSD) depends on the rain rate. Therefore, we have to transform our empirical relationship between KEF and $k(600)$ to one between R_n and $k(600)$. One way to accomplish this is to take a relationship between RSD and R_n and calculate KEF as a function of different rain rates. As an example, we chose the relationship developed by Marshall and Palmer (1948) because of its simplicity and because it is one of the most widely observed RSD's in nature. The MP distribution function $N(D)$ can be expressed as:

$$N(D)=N_0 \exp(-41R_n^{-0.21}D), \tag{18}$$

where D is the raindrop diameter in cm, R_n is the natural rain rate (mm h^{-1}), and N_0, the value of $N(D)$ for $D=0$, is 0.08 cm^{-4}. From the MP distribution function, we derive a relationship between KEF and R_n, resulting in the following equation:

$$\mathrm{KEF}=3.43\times10^{-3}R_n^{1.17}, \tag{19}$$

where KEF is expressed in J m^{-2} s^{-1} and R_n is in mm h^{-1}. Combining eq. (19) with our empirical equation relating $k(600)$ to KEF (eq. (17)), we obtain:

$$k(600)=0.929+0.679R_n-0.0015R_n^2. \tag{20}$$

Eq. (20) can then be used to predict $k(600)$ given R_n if the RSD is similar to the MP RSD. In cases where the RSD deviates from the MP RSD, another RSD formulation could be combined with eq. (17) to derive a relationship between R_n and KEF.

5.2. *Comparison with earlier work*

A direct comparison between earlier work on the effect of rain on gas exchange (Banks et al., 1984; Belanger and Korzun, 1991) and our experiments can only be done at rain rates less than 25 mm h^{-1} because of the lack of data at higher rain rates in the earlier studies. At these low rain rates, Belanger and Korzun (1991) estimate a gas transfer velocity that is about 20% higher than that derived from our experiments (Fig. 3a). For low rain rates, the relationship of Banks et al.

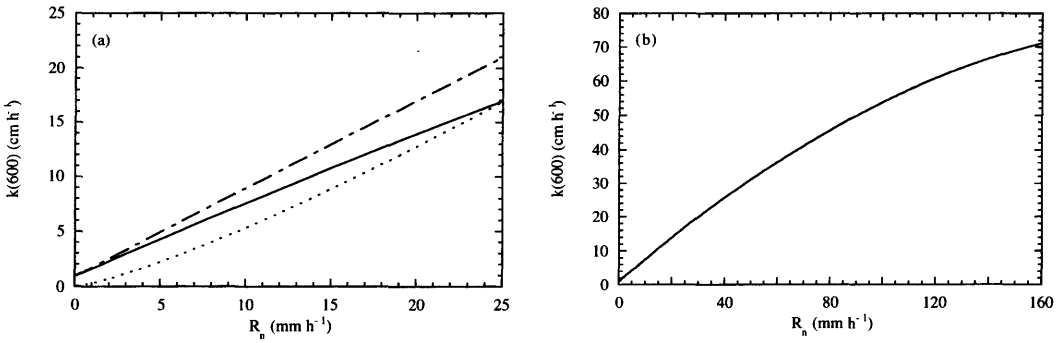

Fig. 3. (a) Comparison of relationships between rain rate R_n and gas transfer velocity $k(600)$ (for R_n between 0 and 25 mm h^{-1}): Dotted line from Banks et al. (1984); dashed-dotted line from Belanger and Korzun (1991); solid line from this study (eq. (20)). (b) Relationship between rain rate R_n and gas transfer velocity $k(600)$ derived from the Marshall-Palmer raindrop size distribution (eq. (20)).

(1984) estimate a gas transfer velocity that is lower than that derived from our relationship because they assume $k(600)=0$ for $R_n=0$. From $R_n=$ 5–25 mm h^{-1}, the difference between k (600) predicted from their relationship and ours, decreases almost linearly (from 45%) until they intercept at $R_n=25$ mm h^{-1} (Fig. 3a).

The laboratory experiments of Banks et al. (1984), were similar to ours, with a few notable exceptions: Their rain simulator had only 12 nozzles, the height of their rain simulator (3.5 m) was not sufficient for raindrops to achieve terminal velocity, they used a mechanical impeller in the water tank to mix the water, and they measured the invasion of O_2 into deoxygenated water, with a correction for the O_2 content of the rain droplets. In their field experiments, Belanger and Korzun, (1991) also measured the invasion of O_2 by filling small circular plastic pools with deoxygenated water and measuring the increase in O_2 as a function of rain rate.

5.3. *Processes responsible for rain induced gas exchange*

We hypothesize that the downward curvature in our $k(600)$ versus R_n curve (Fig. 3b) is due to the fact that gas exchange across the air-water interface is a competing interaction between molecular and turbulent exchange near the water surface and vertical mixing in the water. Normally, the rate of vertical mixing is fast compared to gas exchange across the air-water interface. However, at high rain rates, and hence high gas exchange rates, vertical mixing becomes comparatively slower and thus might emerge as the rate limiting process. The validity of this hypothesis is currently being investigated.

At this time, it is not clear how rain induced turbulence and waves influence gas transfer velocities. However, the fact that gas transfer velocities of the two dropsizes become indistinguishable when expressed in terms of KEF (Fig. 2b) suggests that for these two dropsizes, the physical processes influencing gas exchange are insensitive to dropsize. For equivalent kinetic energy flux to the water surface (pounding of the water surface), the gas exchange rate is similar for a dropsize close to the median size for natural rain (2.8 mm), and a dropsize that is large in natural rain (4.2 mm).

The mechanism behind the enhancement of gas exchange due to rain remains to be examined. Rain should contribute to near-surface turbulence in the water but raindrops also entrain air bubbles which might be a plausible candidate for enhancing gas exchange. Since the effect of bubble-mediated gas exchange is stronger for gases of low solubility (e.g., SF_6) relative to those with higher solubility (e.g., N_2O), multiple gas experiments could be used to determine the relative importance of each effect. If indeed bubbles are responsible for the enhanced gas exchange due to rain, then the relationship derived here using SF_6, because of its low solubility, would represents the maximum effect rain would have on air-water gas exchange. The fact that rain is often colder than the water surface onto which it falls could also be import-

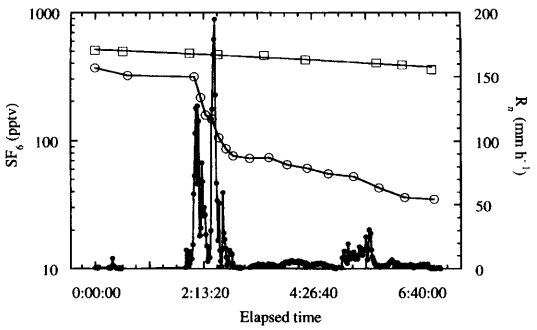

Fig. 4. SF_6 concentration decrease in the two pools with time (log scale) along with the rain rate during the Miami field experiment. Open squares = control; open circles = SF_6 evasion experiment; filled circles = rain rate (1-min averages).

ant. Therefore, future work should pay attention to the contribution of rain to density-driven convection in the water boundary layer. Furthermore, since surfactants tend to impede gas exchange, the effect of rain on dispersing surfactants should be examined. The effect of rain falling on salt water should be considered. For salt water, the enhancement of gas exchange due to rainfall on the water surface could be suppressed by the density stratification created by the rain. Finally, the interaction between rain and wind should be considered. Because of the effect of rain on air-water gas exchange shown here and the fact that rain can enhance the wind stress acting on the water surface (Caldwell and Elliott, 1972), rain will almost certainly have an effect on wind-induced gas exchange. Yet, the combined effect is probably not a simple addition of the two individual processes. Further studies should examine the combined effect of rain and wind on air-water gas exchange.

5.4. *Comparison to field data*

During a tropical rainstorm in Miami, Florida, an SF_6 evasion experiment was performed in a similar fashion as those described above. Two round water pools (diameter = 136 cm; height = 30 cm) were placed next to each other. One of them was sheltered from the rain by a canopy suspended at a height of 3 m to provide the control experiment. Fig. 4 shows the SF_6 concentration decrease in the two pools with time along with the rain rate. The rain rate was measured with a capacitance rain gauge, and RSD was obtained on a Joss-Waldvogel disdrometer (Nystuen et al., 1994).

The kinetic energy flux of the Miami rain was calculated from the measured RSD and related to $k(600)$. Most of the rain events during this storm exhibited the MP RSD. The comparison of field data from Miami with the laboratory data from RSIF shows good agreement between controlled laboratory experiments and field observations (Fig. 5a). To determine the robustness of the transformation using KEF from MP RSD, we plot, in Fig. 5b, the rain rate versus gas exchange for the Miami experiment along with the relationship calculated from eq. (20). Again, there is good agreement between the laboratory data from RSIF and the field data from Miami. Both data sets show a significant increase in $k(600)$ with either increasing KEF or R_n.

6. Conclusions

The gas exchange study conducted at RSIF using SF_6 in gas evasion experiments clearly shows that rain enhances gas exchange. The gas exchange rate can be related to rain rate and dropsize by a single parameter, the kinetic energy supplied to the water surface by the raindrops (kinetic energy flux). Additionally, the relationship between mono-dropsize laboratory rain and gas exchange could be extended to natural rain using the Marshall-Palmer raindrop size distribution (MP RSD). This relationship should hold for most natural rain events as the MP RSD is well established. In cases where the RSD differs dramatically from the MP distribution, other parameterizations could be used instead to estimate the RSD and the KEF could then be calculated accordingly.

The effect of rain on air-water gas exchange is probably most pronounced at sites where wind-driven turbulence is not the dominant contributor to gas exchange. Such sites include wetlands, particularly because most wetlands are sheltered and located in high-precipitation regions. In view of the results presented here and the preliminary studies done in the field showing the dramatic effect that rain can have on air-water gas exchange, more extensive investigations should be consid-

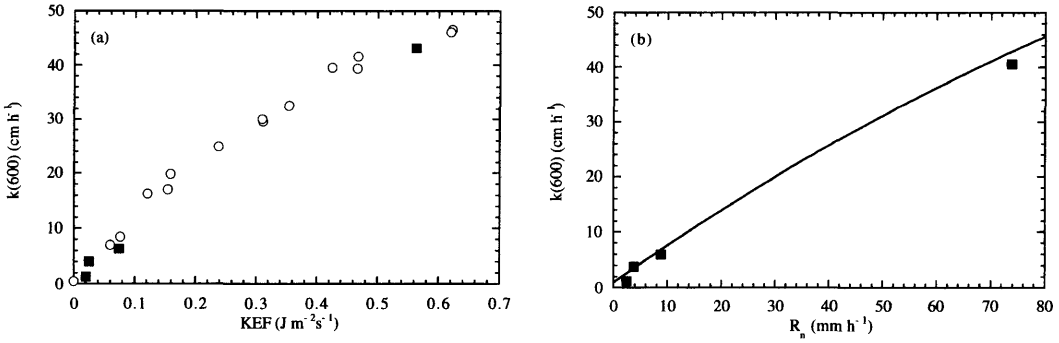

Fig. 5. (a) Comparison of field and laboratory data using the relationship between kinetic energy flux KEF and gas transfer velocity $k(600)$. Open circles = laboratory experiments at RSIF and filled squares = field data obtained in Miami, Florida. (b) Comparison of field and laboratory data using the relationship between rain rate R_n and gas transfer velocity $k(600)$. Line = this study (eq. (20)); squares = field data obtained in Miami, Florida.

ered in natural environments where rainfall might have the greatest effect on gas exchange.

7. Acknowledgements

We thank E. Gordan, M. Lee, and R. Wukitch for help with the experiments at RSIF, M. Boland for providing the Miami rain data, J. Nystuen for discussion of the raindrop size distribution measured in Miami, and H. J. Simpson for constructive comments on the manuscript. Financial support was provided by the NASA Mission to Planet Earth Program through the RTOP 972–461–31–08 and by Columbia University through the Strategic Research Initiative. LDEO contribution no. 5610.

REFERENCES

Banks, R. B., Wickramanayake, G. B. and Lohani, B. N. 1984. Effect of rain on surface reaeration. *J. Envir. Eng.* **110**, 1–14.

Bates, T. M., Kelly, K. C. and Johnson, J. E. 1993. Concentrations and fluxes of dissolved biogenic gases (DMS, CH_4, CO, CO_2) in the Equatorial Pacific during the SAGA 3 experiment. *J. Geophys. Res.* **98**, 16969–16977.

Belanger. T. V. and Korzun E. A. 1991. Rainfall-Re-aeration Effects. In: Air-water mass transfer, *Proceedings of the 2nd International Symposium on Gas transfer at water surfaces* (ed. S. C. Wilhelms and J. S. Gulliver). ASCE, New York, 388–399.

Bliven, L. F. and Elfouhaily, T. M. 1993. Presenting the rain-sea interaction facility. *NASA Reference Publication no. 1322.* NASA-GSFC-WFF, Wallops Island, VA, USA.

Bopp, R. F. 1983. Revised parameters for modeling the transport of PCB components across an air water interface. *J. Geophys. Res.* **88**, 2521–2529.

Bopp, R. F., Santschi, P. H., Li, Y.-H. and Deck, B. L. 1981. Biodegradation and gas-exchange of gaseous alkanes in model estuarine ecosystems. *Organic Geochem.* **3**, 9–14.

Broecker, W. S., Peng, T.-H., Ostlund, G. and Stuiver, M. 1985. The distribution of bomb radiocarbon in the ocean. *J. Geophys. Res.* **99**, 6953–6970.

Caldwell D. R. and Elliott W. P. 1972. The effect of rainfall on the wind in the surface layer. *Bound.-Layer Meteor.* **3**, 146–151.

Clark, J. F., Schlosser, P., Wanninkhof, R., Simpson, H. J., Schuster, W. S. F. and Ho, D. T. 1995a. Gas transfer velocities for SF_6 and ^3He in a small pond at low wind speeds. *Geophys. Res. Lett.* **22**, 93–96.

Clark, J. F., Simpson, H. J., Bopp, R. F. and Deck, B. L. 1995b. Dissolved oxygen in the lower Hudson estuary: 1978–93. *J. Envir. Eng.* **121**, 760–763.

Dyrssen, D., Fogelqvist, E. and Krysell, M. 1990. Release of halocarbons from an industrial estuary. *Tellus* **42B**, 162–169.

Gunn, K. L. S. and Kinzer, G. D. 1949. The terminal velocity of fall for water droplets in stagnant air. *J. Meteor.* **6**, 243–248.

Jähne, B., Münnich, K. O., Bösinger, R., Dutzi, A., Huber, W. and Libner, P. 1987. On parameters influencing air-water gas exchange. *J. Geophys. Res.* **92**, 1937–1949.

King, D. B. and Saltzman, E. S. 1995. Measurement of the diffusion coefficient of sulfur hexafluoride in water. *J. Geophys. Res.* **100**, 7083–7088.

Livingstone, M. D. and Imboden, D. M. 1993. The non-linear influence of wind-speed variability on gas transfer in lakes. *Tellus* **45B**, 275–295.

Marshall, J. S. and Palmer, W. M. 1948. The distribution of the raindrops with size. *J. Meteor.* **5**, 165–166.

McConnell, L. L., Cotham, W. E. and Bidleman, T. F. 1993. Gas exchange of Hexachlorocyclohexane in the great lakes. *Environ. Sci. Technol.* **27**, 1304–1311.

Merlivat, L. and Memery, L. 1983. Gas exchange across an air–water interface: experimental results and modeling of bubble contribution to transfer. *J. Geophys. Res.* **88**, 707–724.

Nystuen, J. A., Proni, J. R., Lauter Jr, C. A., Bufkin, J., Rivero, U., Boland, M. and Wilkerson, J. C. 1994. APL disdrometer evaluation. *NOAA Technical Memorandum ERL AOML-83 (PB95–181681).* Miami, FL, USA.

O'Connor, D. J. 1962. Organic pollution of the New York harbor. Theoretical considerations. *J. Water Poll. Control Fed.* **34**, 905–919.

Odum, H. T. 1956. Primary production in flowing waters. *Limnol. Oceanogr.* **1**, 102–117.

Sobieski, P. W. and Bliven, L. F. 1995. Scatterometry of a drop impact on a salt water surface. *Int. J. Remote Sensing* **16**, 2721.

Thomann, R. V., Mueller, J. A., Winfield, R. P. and Huang, C.-R. 1991. Model of fate and accumulation of PCB homologues in Hudson Estuary. *J. Envir. Eng.* **117**, 161–178.

Upstill-Goddard, R. C., Watson, A. J., Liss, P. S. and Liddicoat, M. I. 1990. Gas transfer in lakes measured with SF_6. *Tellus* **42B**, 364–377.

Wanninkhof, R. 1992. Relationship between gas exchange and wind speed over the ocean. *J. Geophys. Res.* **97**, 7373–7381.

Wanninkhof, R. and Bliven, L. 1991. Relationship between gas exchange, wind speed and radar backscatter in a large wind-wave tank. *J. Geophys. Res.* **96**, 2785–2796.

Wanninkhof, R., Ledwell, J. R. and Broecker, W. S. 1985. Gas exchange — wind speed relationship measured with sulfur hexafluoride on a lake. *Science* **227**, 1224–1226.

Wanninkhof, R., Ledwell, J. R., Broecker, W. S. and Hamilton, M. 1987. Gas exchange on Mono Lake and Crowley Lake, California. *J. Geophys. Res.* **92**, 14567–14580.

Yvon, S. A. and Butler, J. H. 1996. An improved estimate of the oceanic lifetime of atmospheric CH_3Br. *Geophys. Res. Lett.* **23**, 53–56.